Synthesis of Photoisomeric Azobenzene Monomers and Model Compound Effect on Electric–Optical Properties in PDLC Films

Jui-Hsiang Liu, Fuh-Tsang Wu

Department of Chemical Engineering, National Cheng Kung University, Tainan, 70101 Taiwan, Republic of China

Received 4 May 2004; accepted 2 June 2004
DOI 10.1002/app.21021
Published online in Wiley InterScience (www.interscience.wiley.com).

ABSTRACT: A series of azobenzene monomers and related model compounds with various side-chain lengths were synthesized. The electrooptical properties of a polymer-dispersed liquid crystal (PDLC) were verified by side-chain methoxy azobenzene in various chain lengths (n = 3, 6, 11). The properties under various voltages were measured and the effect of extra voltage on the transmittance of PDLC was researched as well. The experiment demonstrated the validity of employing these side chain methoxy azobenzene materials in electrooptical devices. The azobenzene model compound showed better electric–optical and thermal–optical properties, having a higher contrast ratio (CR = 689) and a lower saturation voltage (4.7 V/μm). All the azobenzene molecules can be photoisomerized through UV light irradiation, following the mechanism of isomerization. The reversible photo and heat isomerization property was studied. The *cis*-azobenzene that was transformed from the *trans*-azobenzene irradiated by UV light can decrease the clearing point of the liquid crystal phase. We used this unique characteristic to record image patterns and it worked successfully. We synthesized the azobenzene monomers can stabilize the PDLC and their relative model compounds with various alkyl chain lengths even got better electric–optical effects. We found that azobenzene monomer shows different behaviors in the electric–optical property from its relative model compound. The difference between the systems were explained using a proposed model. © 2005 Wiley Periodicals, Inc. J Appl Polym Sci 97: 721–732, 2005

Key words: monomers; films; light scattering; radical polymerization; optical properties

INTRODUCTION

In the advanced materials field, liquid–crystal polymer composites have been widely studied in the last two decades because of potential applications such as switchable windows, displays, color projectors, and other electric–optical systems.[1–5] This new type of material has been successfully proposed and has received a great deal of attention owing to its electric–optical properties, which are useful in the design integrated optical structures and electric–optical devices. This composite material is known as polymer-dispersed liquid crystal (PDLC) films and consists of micron-sized nematic liquid-crystal (LC) droplets dispersed in a polymeric matrix. In fact, due to the refractive indices mismatch of LC droplets and of the polymeric matrix, PDLC samples appear opaque at room temperature and in the absence of any external electric field. To exploit the electric–optical properties of such materials, it is constructive to realize a multilayer consisting of a PDLC film sandwiched between substrates having a transparent conducting electrode, such as indium tin oxide (ITO), to apply an electric field. Upon application of voltage across the electrodes of the sample, the applied electric field aligns the molecular director of LC inside the droplets, so that there is an index matching between the LC and the polymer matrix. As a consequence, this results in a decreasing of the light scattered by the droplets. When the electric field is removed, the film of PDLC returns to the scattering state.

Several methods to disperse the LC droplets in the polymer matrix have been reported:[6]

1. Polymerization induced phase separation (PIPS): The liquid crystal is dissolved in the prepolymer followed by either thermally or photochemically polymerization.
2. Thermally induced phase separation (TIPS): The liquid crystal is dissolved in the polymer melt followed by cooling.
3. Solvent induced phase separation (SIPS): The liquid crystal is dissolved with the polymer in a common solvent followed by evaporation of the solvent.

The dye in the PDLC can be a dichroic dye that has been used extensively in guest–host display systems.

Correspondence to: J. H. Liu (jhliu@mail.ncku.edu.tw).

Although isotropic dyes are usable, dichroic dyes are preferred because dichroic dyes dissolved in the LC droplets produce a higher color contrast than is possible utilizing isotropic dyes. The absorption of the dichroic dye aligned by nematic LC droplets is modulated by an electric field. In the OFF-state, the alignment of the dichroic dye varies randomly from droplet to droplet with the effect that the extinction coefficient averaged over all droplets is equal to the isotropic extinction coefficient of the dye. In the ON-state the dichroic dye in the droplets is aligned normally to the film surface, and the dye extinction coefficient is equal to the perpendicular extinction coefficient. Therefore, the dye dissolved in the droplet exhibits dichroic properties, which improve the contrast of the PDLC display.[7,8] Dichroic dye employed in a PDLC film produces a higher contrast than an isotropic dye; Lee et al.[8] used an azo dye in a PDLC system by using a circularly polarized light to align the azo dye along the applied field direction so as to enhance the contrast of PDLC.

Several types of liquid crystal–polymer composites present memory effects such as found with different UV-curable materials,[9] surface molecular reorientation,[10] or with smectic liquid crystals.[11] We found the sample with azobenzene component had a memory effect.

Compounds containing photochromic moieties that isomerize under UV irradiation may produce photoinduced conformational changes of the whole macromolecule, in terms of secondary and tertiary structures.[12–14] The azobenzene moiety has been used as a photochromic mesogene in the field of photoelectronics, memory devices, holography, etc.

In this article we present experimental results on the electric–optical properties of PDLC samples prepared in our laboratory, consisting of nematic liquid–crystal domains in a polymer matrix. We use the isomerization property of azobenzene molecules in the PDLC films to record images and the image can be erased by heat; the electric–optical properties of the sample cells were also studied.

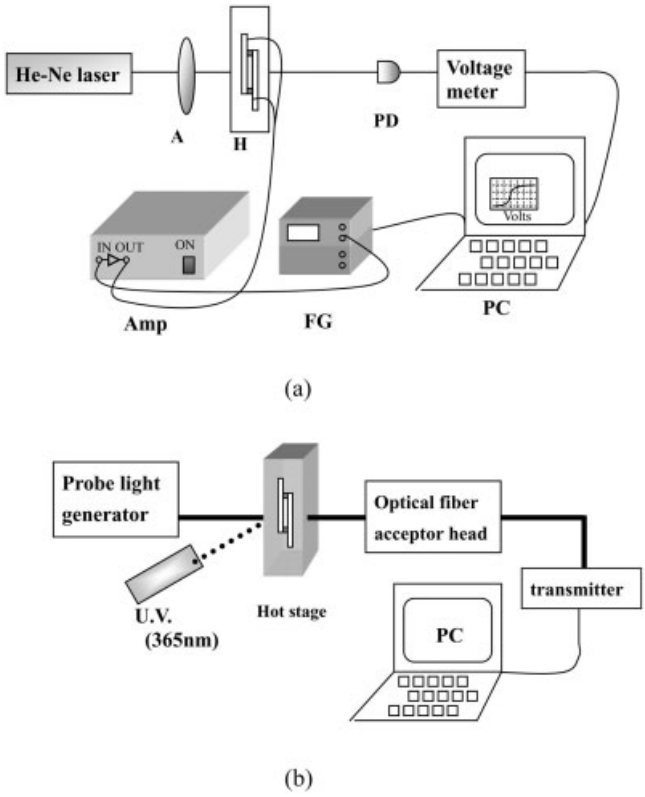

Figure 1 Experimental setup for measurement of electric–optical properties: (a) Amp: amplifier, A: attenuator, FG: function generator, H: sample holder, PD: photodiode; (b) experimental setup for the measurement of the photochemical phase transition behavior.

EXPERIMENTAL

Measurement

Compounds in this study were analyzed by the following instruments. FT-IR spectra were recorded on a Jasco VALOR III Fourier Transforms Infrared spectrophotometer (Tokyo, Japan). Nuclear magnetic resonance (NMR) spectra were obtained on a Bruker AMX-400 high-resolution NMR spectrometer (Darmstadt, Germany). Elemental analyses were conducted with a Heraeus CHN (Darmstadt, Germany) rapid elemental analyzer. Compound decomposition temperature (T_d) was evaluated by thermogravimetric analyzer (TGA-7, Perkin–Elmer Cetus Instrument, USA). Thermal properties analyses of the methoxy azobenzene derivatives were analyzed by Perkin–Elmer differential scanning calorimetry, DSC-7, at a second heating and cooling rate of 10 K/min in nitrogen atmosphere. The liquid crystal phase was invastigated by an Olympus BH-2 (Osaka, Japan) polarized optical microscope (POM) equipped with Mettler hot stage (Model FP-82; Greifensee, Switzerland) and the temperature was controlled in the range of the liquid crystal phase of each compound. SEM photographs were taken by using a multifunction Scanning Electron Microscope, Jeol JXA-840 (Tokyo, Japan).

The electric voltage versus transmittance was then analyzed using the equipment shown in Figure 1(a). The light source was a He-Ne laser passed through an attenuator (A) and the sample film hold on a holder (H). A photodiode (PD) detector placed immediately behind the sample detected the transmitted light and was connected to a voltage meter, which translated the signal and recorded it on the computer. The computer sent a continuous voltage signal (0–7 V) through a function generator (1 kHz), then connected to an amplifier (20-fold) and then applied a voltage to the PDLC sample.

Thermal–optical analysis was performed using the experimental apparatus in Figure 1(b). The sample was placed in a programmable hot-stage that allowed temperature control to ± 0.4°C. A heating rate of 2.0°C/min was used throughout. The probe light source with a halogen lamp was chosen with a 632 nm wavelength and a 2.0 nm bandwidth as the probe light. The probe light was passed through the sample that was clipped inside the hot-stage and then the light passed through an optical fiber acceptor head connected with an optical fiber. The intensity of the probe light was translated into an electric signal and then recorded by the computer. The UV source was 365 nm, Model UVL-56, UVP (Tokyo, Japan), 0.2 mW/cm^2 irradiated at the sample at an angle of 45°.

The light intensity passing through with an empty cell was defined as 100% transmittance. Properties defined as follows: V_{10}, V_{90} are the voltages necessary to obtain a transmission of 10 and 90%; T_{10} is the temperature when the transmittance is 10% and $T_{N\text{-}I}$ is the temperature when the transmittance is up to its maximum transmittance; temperature hysteresis (ΔT_{50}) measured the temperature difference between the thermal–optical curves obtained before and after UV irradiation of 50% transmission. The contrast ratio (CR) of the film was defined as $CR = T_{max}/T_{min}$, where T_{max} and T_{min} are the maximum and minimum transmittance, respectively.

The morphology of cured PDLC film was examined using a scanning electron microscope (SEM) with a JEOL JSM-35 instrument (Osaka, Japan). The peeled-off sample was submerged into *n*-hexane and then washed under supersonic for 1 h. The liquid crystal molecules, unreacted monomer, and inert component were then extracted, dried in vacuum at 30°C, and coated with gold film.

Materials

The liquid crystal we used was E7, purchased from Merk (Darmstadt, Germany). Its components were an eutectic mixture of four liquid crystals, where the nematic property ranged from −20 ~ 61°C. Ethylene glycol dimethacrylate (EGDMA) as crosslinking monomer was purchased from Acros (Geel Belgium). Azobisisobutyronitrile (AIBN) purified from acetone used as thermal initiator was purchased from Acros.

All the chemicals were purchased from commercial suppliers and used without further purification except for the acylation process. The dioxane was dried with sodium. After distillation it was then stored in a brown bottle with 4 Å molecular sieves before being used.

Synthesis and characterization of azobenzene molecules

4-Hydroxy-4′-methoxy-azobenzene

p-Anisidine (10 g, 81.20 mmol) was dissolved in 1.5*M* aqueous HCl (100 mL) and kept in an ice bath at 0°C. Sodium nitrite (6 g, 86.96 mmol) in water (20 mL) was added dropwise to the former solution and stirred for 1 h. Sodium hydroxide (8.4 g, 0.21 mol) and phenol (8.4 g, 89.26 mmol) were dissolved in water (80 mL) and stirred at −2°C. The former solution was added dropwise to the latter solution at −2°C and then stirred for 1 h. The resulting mixture was poured into water and the solution was acidized with 2*M* aqueous HCl to pH 2. The crude was washed with water twice until neutral and recrystallized from ethanol. Yield: 14.74 g (80%), yellow crystalline powder.

FTIR (KBr, cm^{-1}): 3419 (OH). ^{1}H-NMR, $CDCl_3$, δ (ppm): 6.92–7.88 (m, 8H, aromatic), 3.9 (s, 3H, $ArOCH_3$).

1-Hydroxy-3-(4-methoxy-azobenzene-4′oxy)propane (M3H)

Compound 4-Hydroxy-4′-methoxy-azobenzene (4.0 g, 17.52 mmol) was dissolved in ethanol (200 mL). KOH (1.12 g, 19.96 mmol) and a trace of KI dissolved in 30 mL water was added dropwise to the former solution; 1-chloro-propanol (1.82 g, 19.25 mmol) dissolved in ethanol (20 mL) was then added. The solution was refluxed at 90°C for 24 h. The resulting mixture was poured into water and extracted with diethylether. The water phase was collected and acidized to pH 2 and then washed with neutral water until neutral. The crude was filtered and recrystallized from ethanol. Yield: 4.06 g (81%), yellow crystalline.

FTIR (KBr, cm^{-1}): 3280 (OH), 2948, 2872 (CH_2). ^{1}H-NMR, $CDCl_3$, δ (ppm): 6.99–7.89 (m, 8H, aromatic), 4.19–4.22 (t, 2H, OCH_2), 3.9 (s, 3H, $ArOCH_3$), 3.8–3.89 (t, 2H, OCH_2), 2.07–2.10 (m, 2H, $CH_2CH_2CH_2$).

1-Hydroxy-6-(4-methoxy-azobenzene-4′oxy)hexane (M6H)

Compound M6H was similarly synthesized as M3H. Yield: 66%, yellow crystalline.

FTIR (KBr, cm^{-1}): 3300 (OH), 2938, 2864 (CH_2). ^{1}H-NMR, acetone-d_6, δ (ppm): 7.06–7.87 (m, 8H, aromatic), 4.08–4.11 (t, 2H, OCH_2), 3.89 (s, 3H, $ArOCH_3$), 3.52–3.55 (t, 2H, OCH_2), 1.44–1.83 (m, 8H, $CH_2(CH_2)_4CH_2$).

1-Hydroxy-11-(4-methoxy-azobenzene-4′oxy)undecane (M11H)

Compound M11H was similarly synthesized as M3H. Yield: 71%, yellow cystalline.

FTIR (KBr, cm^{-1}): 3301 (OH), 2917, 2849 (CH_2). ^{1}H-NMR, acetone-d_6, δ (ppm): 7.06–7.87 (m, 8H, aromatic), 4.07–4.11 (t, 2H, OCH_2), 3.88 (s, 3H, $ArOCH_3$), 3.47–3.51 (t, 2H, OCH_2), 1.24–1.82 (m, 18H, $CH_2(CH_2)_9CH_2$).

3-(4-Methoxy-4′-oxy-azobenzene)propyl acrylate (M3E)

Compound M3H (5.23 g, 18.3 mmol), *N*,*N*-dimethylaniline (2.98 g, 24.6 mmol), and a catalytic amount of 2,6-di-*tert*-butyl-*p*-cresol were dissolved in distilled 1,4-dioxane (30 mL). The solution was cooled with an ice bath and then acryloyl chloride (2 mL, 24.6 mmol), dissolved in distilled dioxane (30 mL), was added dropwise under vigorous stirring for 2 h. The mixture was stirred for 24 h at 55°C. After completing the reaction, the solution was poured into ice water and recrystallized twice from ethanol. Yield: 2.18 g (53%), yellow crystalline powder.

FTIR (KBr, cm^{-1}): 2931, 2879, 2838 (CH_2), 1728 (C=O), 1635 (C=C). ^{1}H-NMR, $CDCl_3$, δ (ppm): 6.98–7.89 (m, 8H, aromatic), 6.39–6.45, 5.82–5.86(d, 2H, CH_2=CH), 6.09–6.18 (m, 1H, CH_2=CH), 4.36–4.40 (t, 2H, OCH_2), 4.12–4.16 (t, 2H, OCH_2), 3.88 (s, 3H, $ArOCH_3$), 2.16–2.24 (m, 2H, $CH_2CH_2CH_2$).

$C_{18}H_{18}N_2O_4$ (270) Calcd. C: 67.05, H: 5.92, N: 8.23; Found C: 66.74, H: 5.99, N: 8.20.

6-(4-Methoxy-4′-oxy-azobenzene)hexyl acrylate (M6E)

Compound M6H was similarly synthesized as M3E. Yield: 86%, yellow crystalline.

FTIR (KBr, cm^{-1}): 2940, 2863 (CH_2), 1716 (–C=O), 1631 (C=C). ^{1}H-NMR, $CDCl_3$, δ (ppm): 6.97–7.88 (m, 8H, aromatic), 6.38–6.43, 5.80–5.83 (d, 2H, CH_2=CH), 6.09–6.16 (m, 1H, CH_2=CH), 4.16–4.20 (t, 2H, OCH_2), 4.02–4.05 (t, 2H, OCH_2), 3.88 (s, 3H, $ArOCH_3$), 1.47–1.85 (m, 8H, $CH_2(CH_2)_4CH_2$).

$C_{22}H_{26}N_2O_4$ (382) Calcd. C: 69.09, H: 6.85, N: 7.32; Found C: 68.25, H: 6.91, N: 7.30.

11-(4-Methoxy-4′-oxy-azobenzene)undecyl acrylate (M11E)

Compound M6H was similarly synthesized as M3E. Yield: 88%, yellow crystalline.

FTIR (KBr, cm^{-1}): 2920, 2850 (CH_2), 1722 (C=O), 1637 (C=C). ^{1}H-NMR, acetone-d_6, δ (ppm): 7.05–7.87 (m, 8H, aromatic), 6.29–6.35, 5.83–5.87 (d, 2H, CH_2=CH), 6.08–6.17 (m, 1H, CH_2=CH), 4.07–4.13 (m, 4H, OCH_2), 3.88 (s, 3H, $ArOCH_3$), 1.32–1.85 (m, 18H, $CH_2(CH_2)_9CH_2$).

$C_{27}H_{36}N_2O_4$ (452) Calcd. C: 71.65, H: 8.01, N: 6.19; Found C: 70.41, H: 7.97, N: 6.12.

4-Propyloxy-4′-methoxy-azobenzene (M3C)

Compound 4-hydroxy-4′-methoxy-azobenzene (3.3 g, 14.58 mmol) was dissolved in *N*,*N*-dimethyl formamide (40 mL). Potassium carbonate (6.35 g, 45.94 mmol) dissolved in 15 mL water was added to the solution; 1-bromo-propane (1.96 g, 15.94 mmol) dissolved in *N*,*N*-dimethyl formamide (30 mL) was then added dropwise to the solution. The solution was reacted at 120°C for 24 h. The resulting mixture was poured into ice water and washed with water twice until neutral. The crude was filtered and recrystallized from ethanol. Yield: 4.06 g (81%), yellow crystalline.

FTIR (KBr, cm^{-1}): 2965, 2933, 2877 (CH_2). ^{1}H-NMR, acetone-d_6, δ (ppm): 1.02–1.06 (m, 3H, CH_3–), 1.79–1.84 (q, 2H, –CH_2–), 3.89 (d, 3H, $ArOCH_3$), 4.03–4.07 (m, 2H, OCH_2), 7.07–7.11 (m, 4H, Ar–O), 7.84–7.88 (m, 4H, Ar–N). $C_{18}H_{18}N_2O_2$ (270).

Calcd. C: 71.09, H: 6.71, N: 10.36; Found C: 71.08, H: 6.69, N: 10.36.

4-Hexyloxy-4′-methoxy-azobenzene (M6C)

Compound M6C was similarly synthesized as M3C. Yield: 84%, yellow crystalline.

FTIR (KBr, cm^{-1}): 2937, 2861 (CH_2). ^{1}H-NMR, acetone-d_6, δ (ppm): 0.88–0.92 (m, 3H, CH_3–), 1.34–1.82 (m, 8H, –CH_2–), 3.89 (s, 3H, $ArOCH_3$), 4.08–4.11 (t, 2H, OCH_2), 7.06–7.10 (m, 4H, Ar–O), 7.84–7.89 (m, 4H, Ar–N). $C_{19}H_{24}N_2O_2$ (312).

Calcd. C: 73.05, H: 7.74, N: 8.97; Found C: 72.90, H: 7.73, N: 8.97.

4-Dodecyloxy-4′-methoxy-azobenzene (M12C)

Compound M12C was similarly synthesized as M3C. Yield: 78%, yellow crystalline.

FTIR (KBr, cm^{-1}): 2956, 2918, 2850 (CH_2). ^{1}H-NMR, acetone-d_6, δ (ppm): 0.87–0.85 (d, 3H, CH_3–), 1.23–1.83 (m, 20H, –CH_2–), 3.89 (s, 3H, $ArOCH_3$), 4.08–4.11 (t, 2H, OCH_2), 7.07–7.09, 6.84–6.85 (d, 4H, Ar–O), 7.85–7.88 (m, 4H, Ar–N).

$C_{25}H_{36}N_2O_2$ (397) Calcd. C: 75.72, H: 9.15, N: 7.06; Found C: 75.75, H: 9.12, N: 7.08.

PDLC cell fabrication

Unless otherwise indicated, the composition of the syrup used to make the PDLC films was 80 wt % liquid crystal and 20 wt % prepolymer. The prepolymer EGDMA/azobenzene was 4.5/1 in molar ratio and the initiator was 1.5 mol % with the equivalent molar content of double bond. The presyrup was well mixed with supersonic for 2 h. The liquid crystal and the acrylate mixture were combined to form a single phase. The isotropic fluid was then poured into a sandwiched ITO glass cell with a 15-μm spacer. The

presyrup was polymerized at 90°C for 1 h to form PDLC films and used as the sample for the later electric– and thermal–optical study.

RESULTS AND DISCUSSION

Azobenzene monomers and their relatively low molecular weight model compounds with various alkyl chain length (n = 3, 6, 11, or 12) were synthesized by a similar method to that reported by Angeloni et al.[15] or Silong et al., [16] as shown in Scheme 1 and Scheme 2. The molecular structures were confirmed by FTIR, elemental analysis, and ^{1}H-NMR analyzers.

The results of second heating and cooling differential scanning calorimetry and the compound's decomposition temperature (T_d) were summarized in Table I. The molecules of M3E, M11E, M3C, M6C, M12C, and M6H showed liquid crystalline properties. The enthalpy (ΔH) required for phase transition from smectic (S) to nematic (N) or nematic (N) to isotropic (I) phase was also estimated. Different ΔH values on heating and cooling cycles were observed. The result showed that molecular arrangement and the strength of the intermolecular forces between liquid crystal molecules are different during the cycles. The decomposition temperature (T_d) of the longer alkyl chain azobenzene was higher than the shorter one in the series of ME, MnH, and MnC. The liquid crystalline phases were confirmed by a polarizing optical microscope analyzer. Figures 2 (a)–(d) show the optical textures of M3C, M6H, M3E, and M11E, respectively.

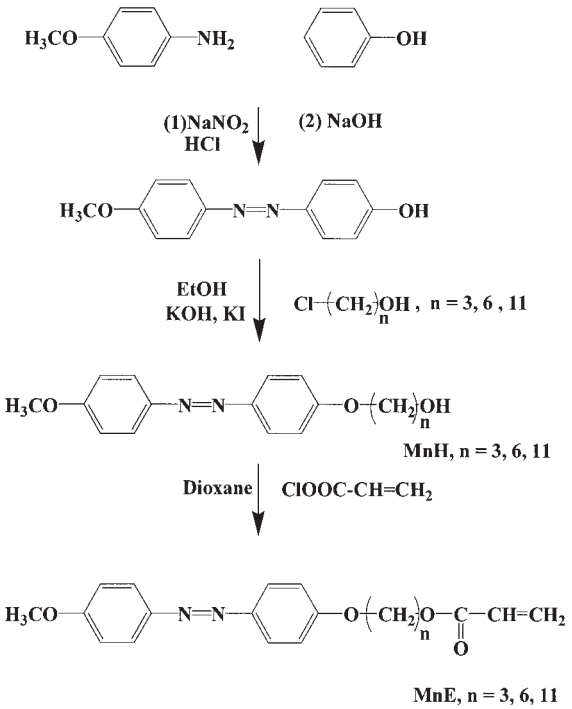

Scheme 1.

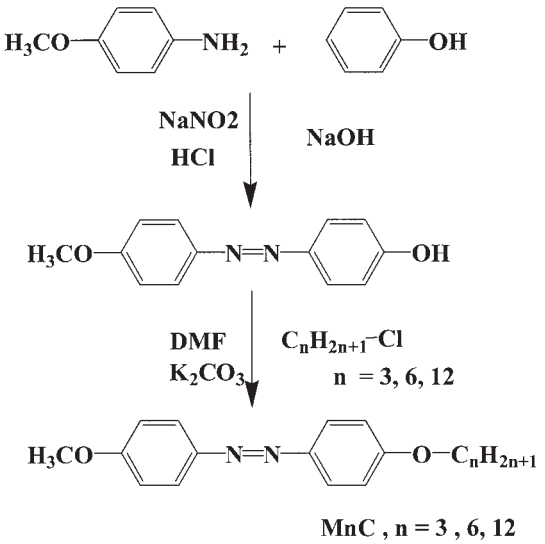

Scheme 2.

Figure 3 shows transmittance versus applied voltage with various contents of E7 ranging from 40 to 80 wt %. As we can see, when we increased the content of liquid crystal, the *CR* was increased. The *CR* was 29 and T_{min} was 3% when the content of prepolymer was 20 wt %. We chose the content of liquid crystal and prepolymer to be 80 and 20 wt % for the later syrup.

Figures 4(a)–(c) show the dependence of transmittance on applied voltage with azobenzene compounds MnE, MnH, and MnC, respectively. Figure 4(a) shows the electric–optical curves of PDLC films containing azobenzene monomer with various alkyl chain lengths (n = 3, 6, and 11); as we can see, the initial transmittance decreased when the alkyl chain length was increased, but the sample still had 15% transmittance of M11E. Figures 4(b) and (c) show the electric–optical curves of PDLC films contained low molecular weight model compounds MnH (n = 3, 6, and 11) and MnC (n = 3, 6, and 12). All of these samples contained low molecular weight azobenzene derivatives that can scatter light well and have a better contrast ratio than azobenzene monomers and the sample didn't contain azobenzene compound. The PDLC that contained M6C had a lower saturation voltage and threshold voltage (V_{10}) than M3C and M12C. We speculated that was because the M6C had a similar molecular alkyl chain length to the liquid crystal we used.

Table II summarized the results of electric–optical properties (V_{10}, V_{90}, ΔV_{50}, T_{OFF}, and *CR*) from Figure 4. The results show that the sample that contained the azobenzene model compound had a much larger *CR* than the sample that contained the azobenzene monomer. The shorter alkyl chain length of MnH and MnC had a higher *CR* and larger alkyl chain length, which decrease threshold voltage and saturation voltage. The longer alkyl chain length in MnC and MnH contained

TABLE I
Thermal Properties of Sample Compounds

Sample	Phase transition for heating cycle		Phase transition for cooling cycle		
	Mesophase[a] (°C)	Enthalpy[b] (J/g)	Mesophase[a] (°C)	Enthalpy[b] (J/g)	T_d[c] (°C)
M3E	K 62 N 81 I	1.05	K 38 N 48 I	−0.98	298
M6E	K 75 N 85 I	—	K 70 I	—	304
M11E	K 66 N 70 I	9.25	K 54 S 60 N 66 I	−13.32, −2.79	310
M3H	K 136 I	—	K 108 I	—	359
M6H	K 119 I	—	K 97 N 106 I	−3.50	360
M11H	K 121 I	—	K 106 I	—	398
M3C	K 108 I	—	K 75 N 90 I	−2.81	276
M6C	K 89 N 95 I	1.05	K 52 N 90 I	−3.17	330
M12C	K 100 I	—	K 84 N 86 I	−1.87	384

[a] K, crystal; S, smectic; N, nematic; I, isotropic.
[b] Enthalpy of phase change during heating and cooling.
[c] Decomposition temperatures of compounds.

PDLC samples with a lower contrast ratio. The contrast ratio can be up to 689 (T_{min} = 0.13, T_{max} = 0.90) for PDLC films containing azobenzene molecule M3C. This is because the sample is highly light scattering of incident light and this leads to a lower transmittance than others as we can see in Figure 4. The contrast ratio is higher than other PDLC systems. Yamaguchi et al.[17] used a urethane mixture in which the *CR* is about 20, Wu et al.[18] rubbed the substrate to create aligned dye-doped PDLC films, enhancing the *CR* up to 28, Petti et al.[2] used epoxy-based PDLC films where *CR* can be up to 410. The longer alkyl chain length decreased the saturation voltage and the threshold voltage.

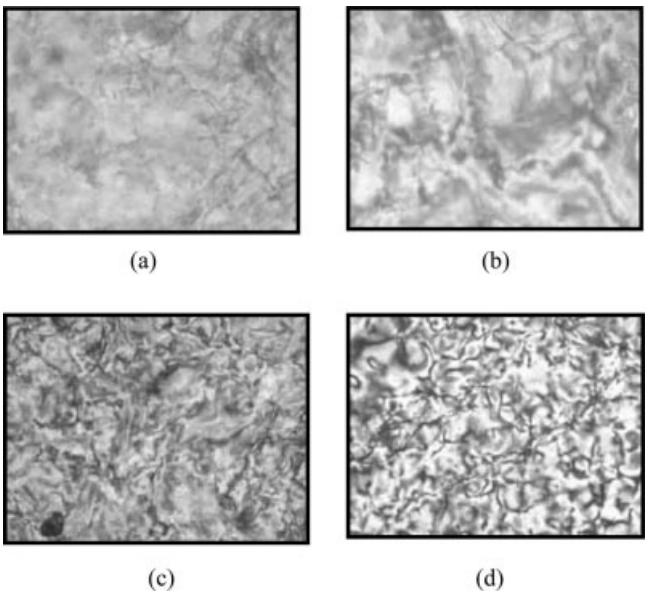

Figure 2 POM textures of azobenzene compounds of (a) M3C, (b) M6H, (c) M3E, and (d) M11E.

Figure 5 shows the absorption in the visible wave length range with various applied voltages of liquid crystal cells that contained azobenzene molecules. As we can see, the transmittance decreased with an increase in the applied voltage. The azobenzene molecules show as a dichroic dye in the liquid, and this is why the PDLC sample that contained azobenzene model compounds shows better contrast ratios than that which contained none.

The SEM photographs show these samples have the polymer ball type morphology.[6,16] The above results show that the azobenzene monomer and its relative model compound have different behavior in the electric–optical characteristic and we proposed a model to explain these phenomena. Figures 6(a)–(d) are the real image analyzed by SEM; the model represents the short alkyl azobenzene monomer, the long alkyl chain azobenzene monomer, and their relative model compounds in the PDLC films, respectively. As we can see

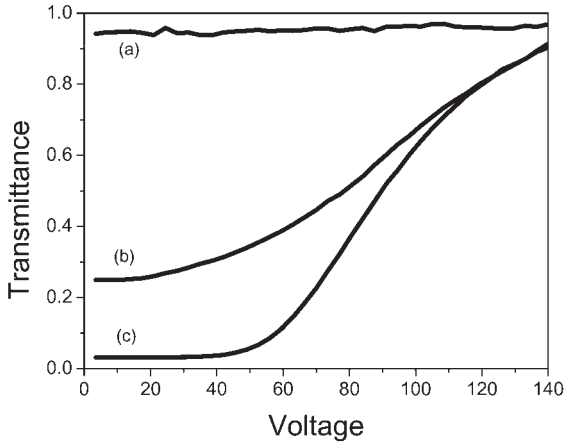

Figure 3 Dependence of transmittance on applied voltage with various contents of E7: (a) 40% (b) 60%, (c) 80%.

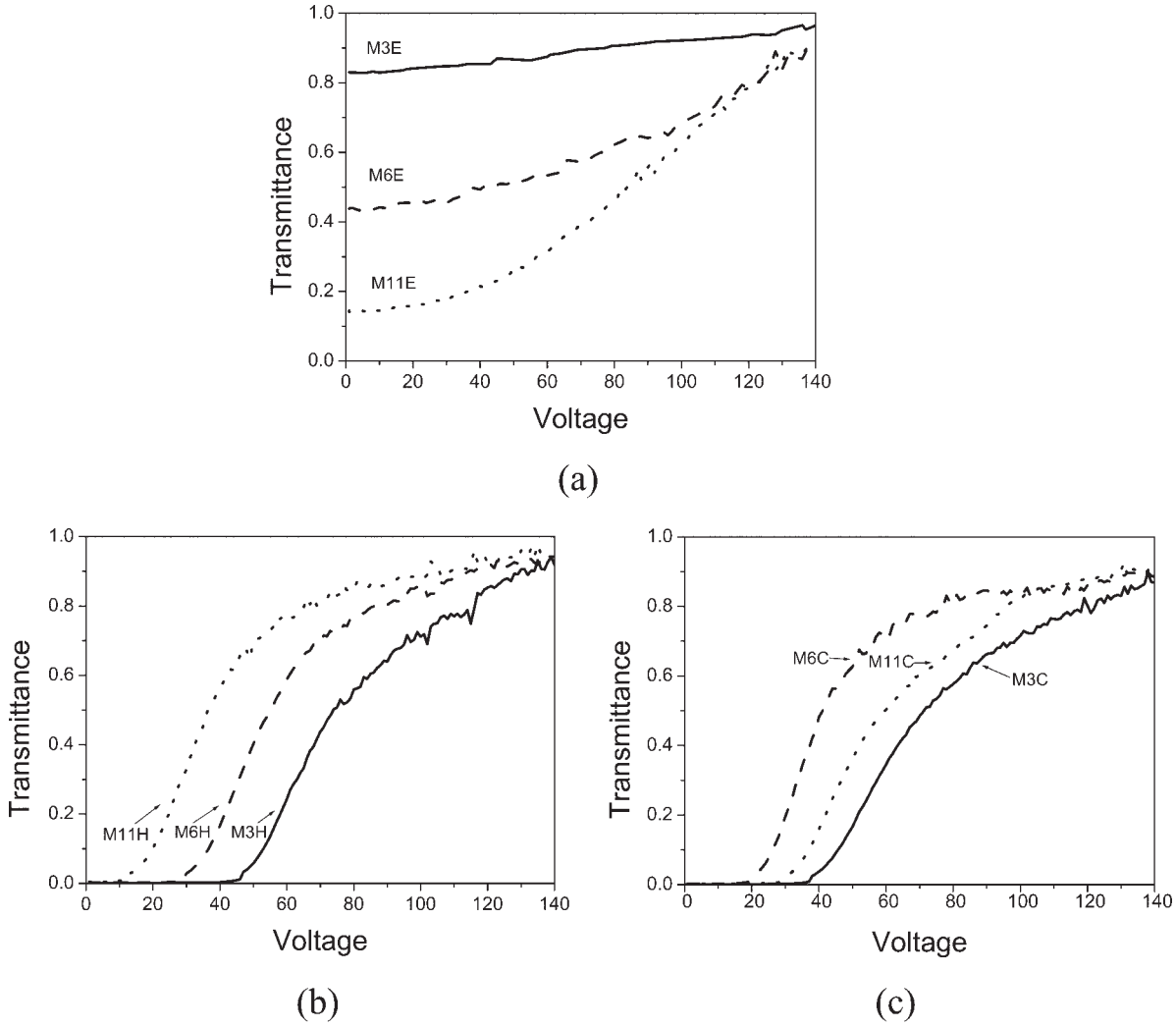

Figure 4 Dependence of transmittance on applied voltage with various azoenzene derivatives, (a) MnE, (b) MnH, and (c) MnC.

in Figure 6(a), the liquid crystal and/or azobenzene molecules were trapped in the channel of the polymer matrix. The liquid crystal domain stated in the model

TABLE II
Electric–Optical Properties of Liquid Crystal Cells with Various Azobenzene Derivatives

Sample	V_{10}(V)[a]	V_{90}(V)[a]	T_{off}(%)[b]	CR[c]
None	58	125	3	29
M3E	—	45	84	1.16
M6E	—	124	48	2.26
M11E	—	124	19	6.27
M3H	45	109	9	689
M6H	26	75	37	330
M11H	36	97	45	272
M3C	53	117	16	616
M6C	36	105	38	523
M12C	20	94	50	198

[a] Applied voltage for 10 or 90% transmittance of cells.
[b] Transmittance after turning off applied voltage.
[c] Contrast ratio, $CR = T_{max}/T_{min}$.

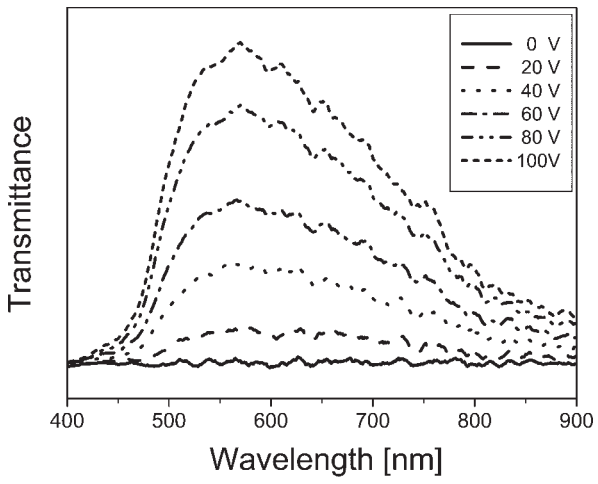

Figure 5 Absorption and wavelength correlation by applied voltage on the azobenzene dye doped liquid crystal samples.

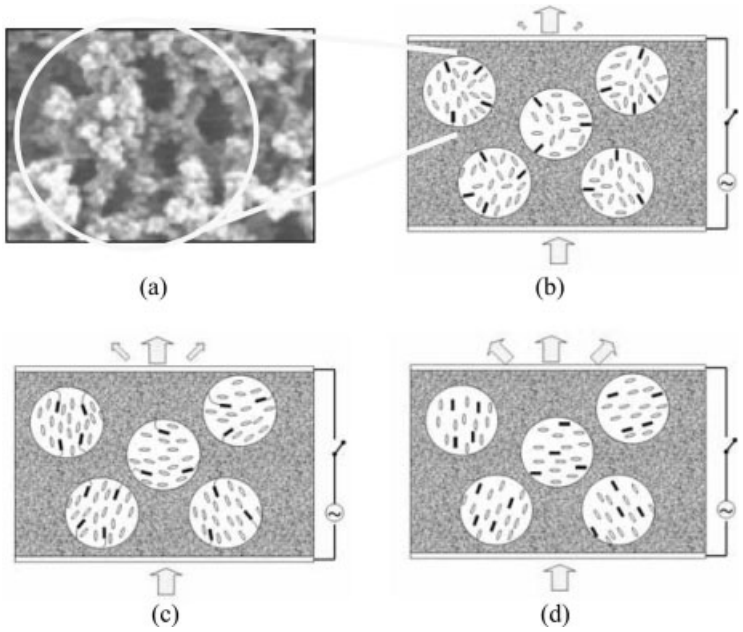

Figure 6 (a) Microstructure of polymer matrix, (b) liquid crystal orientation affected by rigid alkyl side chain, (c) liquid crystal orientation affected by long alkyl side chain, (d) freely orientated liquid crystal molecules in the presence of model azobenzene compounds.

is the average alignment in Figure 6(a). Figure 6(b) shows the short alkyl chain azobenzene monomer (M3E) connected to the polymer matrix; the monomer was rigidly connected to polymer matrix so as to disturb the alignment of the liquid crystal molecules and the alignment of each liquid crystal domain was less aligned to scatter light efficiently. However, the longer alkyl chain azobenzene monomer was more flexible and the azobenzene part penetrated in the liquid crystal molecules as shown in Figure 6(c), liquid crystal molecules aligned more regularly in each liquid crystal domain, and the incident light was refracted when it passed through these birefractive index domains so the sample scattered the incident light much more than the short one. The initial transmittance of samples containing M3E, M6E, and M11E are 83, 44, and 15% respectively, as we can see in Figure 4(a). As Figure 4(d) shows, the azobenzene model compound was more randomly dispersed in the liquid crystal domain than azobenzene monomers and it assisted the liquid crystal molecules to become well aligned in the liquid crystal domain and the birefractive index difference was larger than the monomers so the incident light was highly scattered by these different directions of the liquid crystal domains. The initial transmittance of samples containing MnH or MnC ranged from 0.1 to 0.5%. The model interprets why PDLC samples contain monomers or their relative model compounds that show different initial transmittance.

All *trans*-azobenzene monomers as well as their related low molecular weight model compounds showed, in ethanol solution, a strong UV-vis absorption band centered about 362 nm and a shoulder at around 456 nm attributed to the $\pi \rightarrow \pi^*$ and $n \rightarrow \pi^*$ electronic transitions of the *trans*-azobenzene chromophore, respectively. All samples underwent *trans*-to-*cis* photoisomerization of the azobenzene moiety upon irradiation at 365 nm in the $\pi \rightarrow \pi^*$ absorption region. Figure 7(a) shows the spectrum of the UV-vis absorption of M6H in ethanol solution with various UV light irradiation times and Figure 7(b) shows the UV-vis absorption spectrum in the dark after UV light irradiation for 3 min. The legends show the time. The intensity of the UV-vis absorption bands decreased with irradiation time in the 362 nm region but increased below 325 nm and above 430 nm. The occurrence of two distinct isobestic points at 325 and 430 nm as well as the similarity of the UV-vis spectra of the irradiated samples at the photostationary state with that of *cis*-azobenzene indicate that only two absorbing species (*trans* and *cis* isomers) were present and no side reactions such as photocrosslinking or photodegration occurred. The *trans* to *cis* isomerization required 60 s and recovered to *trans* isomer within 90 min at room temperature. The molar extinction coefficient ε_{max} calculated from the absorbance of λ_{max} is 2.68×10^{-4} /cm/M. The maximum absorption wavelength length of $\pi \rightarrow \pi^*$ and $n \rightarrow \pi^*$ absorption band, molar extinction coefficient, and the two isobestic points were almost the same for all the other azobenzene molecules we studied (MnE, MnH, and MnC). This means that these characteristic properties were

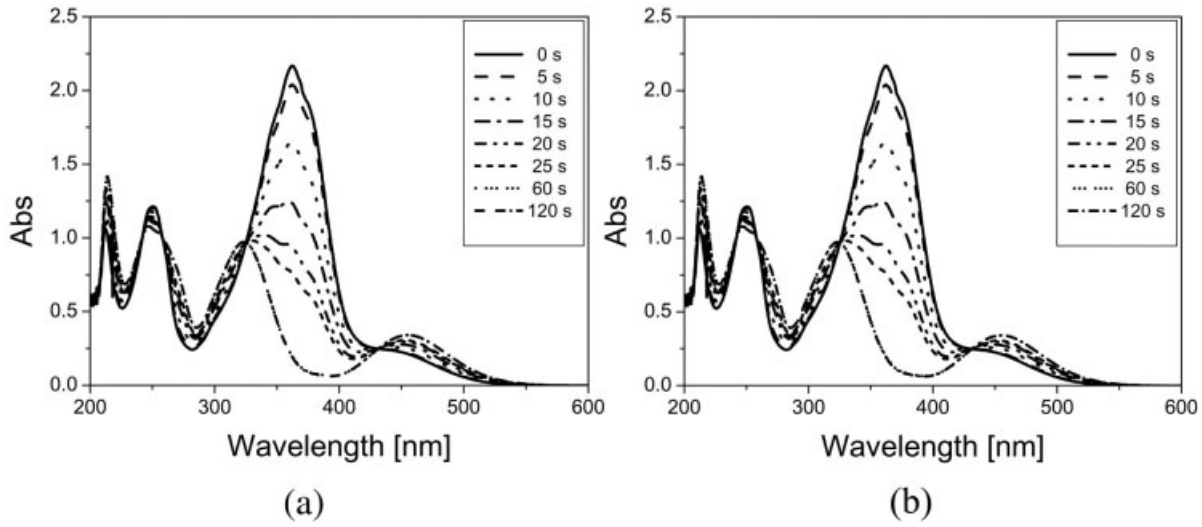

Figure 7 Variation of the UV-vis spectra of M6H (a) with various irradiation times and (b) recovery in dark with various times.

less influenced by the terminal end group (double bound, hydroxy, or methyl) and alkyl chain length.

Figure 8 plots Ar = $\ln[(A_0 - A_\infty)/(A_t - A_0)]$ versus UV (λ = 365 nm) irradiation time for M6H in ethanol, where A_0, A_t, and A_∞ are the absorbance of the sample at time 0, t, and ∞, respectively, show a linear dependence on irradiation time as expected for first order kinetics. The results are consistent with those described in the literature.[19]

Figure 9 describes the model of the phase transition temperature effect through azobenzene isomeriztion reaction. After UV irradiation, the *trans*-azobenzene isomerized to form *cis*-azobenzene so as to disturb the alignment of liquid crystal molecules decreasing the clearing point (T_{NI}) of the liquid crystal. The transmittance of the sample was highly transmitted. The sample can recover to its original highly scattering state by a thermal process. The property of phase transition by UV light can be used to record the image.

Figure 10(a)—(d) shows the dependence of transmittance on various temperatures for PDLC samples containing azobenzene compound M3E, M6E, M3C, and M6C, respectively, before and after UV irradiation. As we can see, the azobenzene monomer was attached to the polymer matrix directly, so it only had an effect near the interface between the polymer matrix and the liquid crystal domain. The effect was restricted so the transmittance is a little higher than initial transmittance after UV light irradiation. The azobenzene model compound dispersed in liquid crystal domain obviously decreased the clearing point. There was a large temperature hysteresis in these samples.

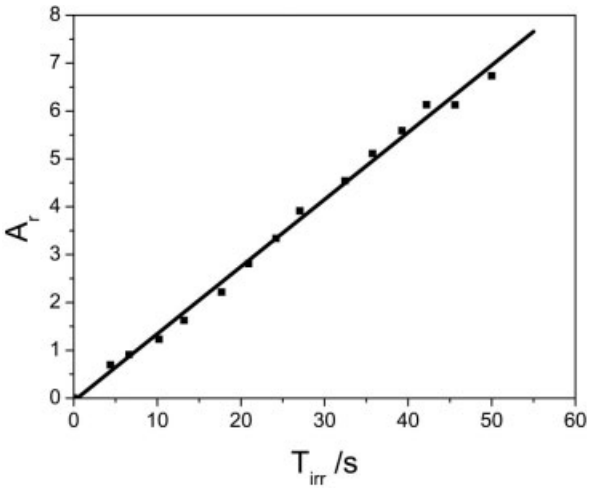

Figure 8 Plot of Ar = $\ln[(A_0 - A_\infty)/(A_t - A_\infty)]$ versus irradiation time for azocompound M6H in ethanol, UV = 365 nm, 0.2 mW/cm^2.

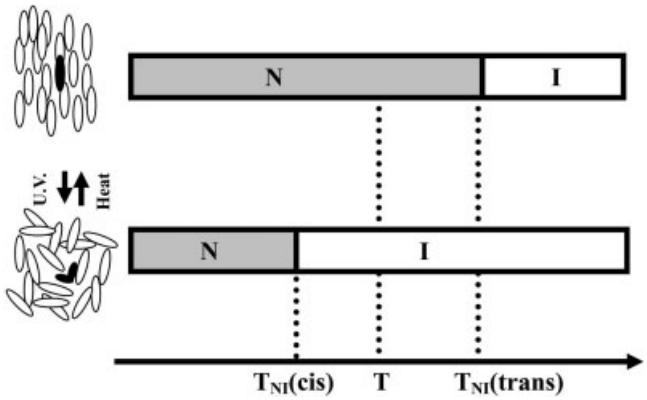

Figure 9 Variation of phase transition temperature of liquid crystal on photoisomerization of azobenzene compounds.

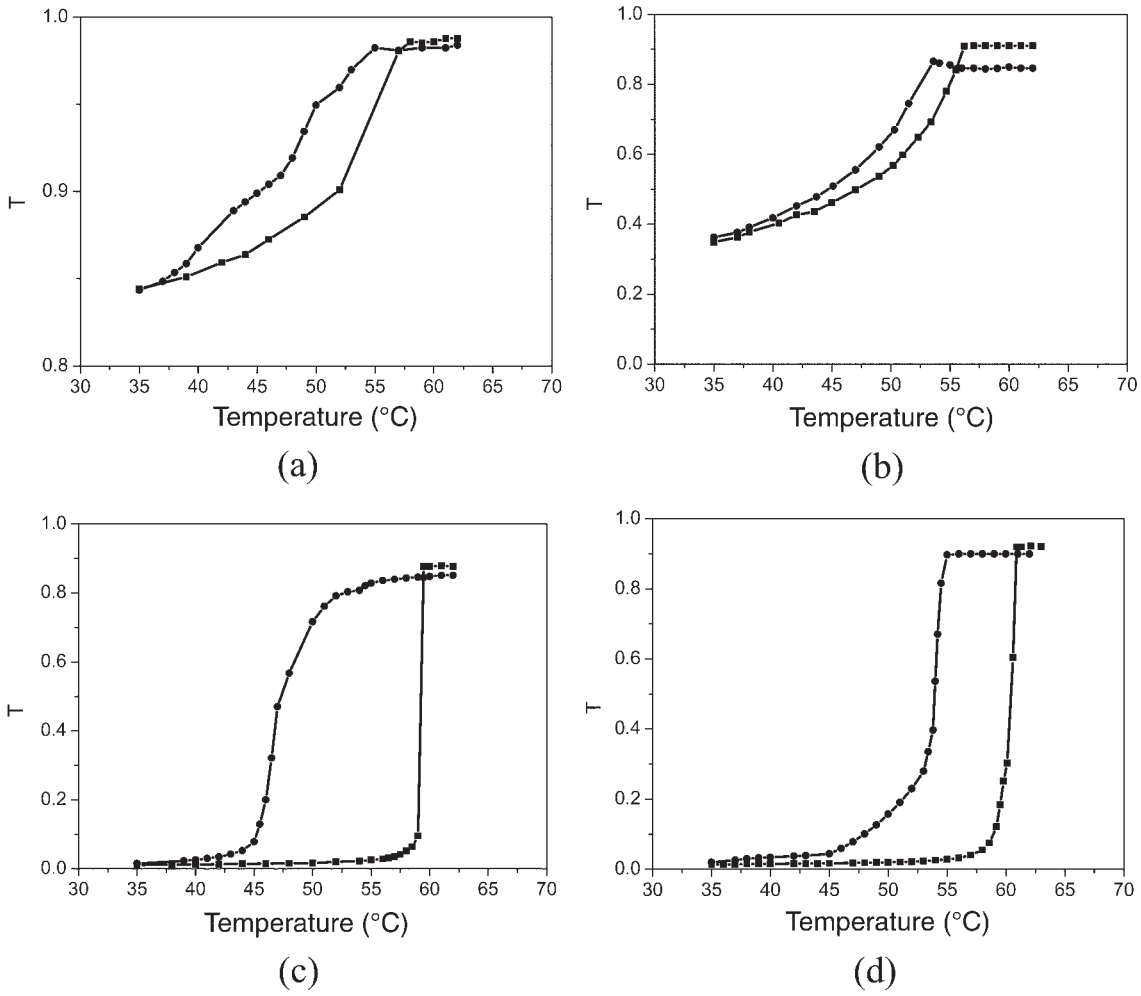

Figure 10 Dependence of transmittance on various temperatures before (■) and after (●) UV irradiation with various azobenzene derivatives of (a) M3E, (b) M6E, (c) M3C, and (d) M6C.

Table III summarizes the value of T_{10}, T_{NI}, and *CR*, before and after UV irradiation and temperature hysteresis (ΔT_{50}). The clearing point of the MnE series was approximately 57°C and for the MnC series was approximately 61°C. This means MnE disturbed the liquid crystal alignment so as to decrease the temperature of the clearing point. The result was coincident with the electric–optical property and the model we

TABLE III
Variation of Thermoproperties of Cell with Various Azobenzene Derivatives Before and After UV Irradiation

	Before UV			After UV			
Sample	T_{10}[a]	T_{NI}[b]	*CR*	T_{10}[a]	T_{NI}[b]	*CR*	ΔT_{50}[c]
M3C	58.5	59.5	79	45	58	56	12
M6C	59	60.9	68	47	55	46	6.5
M12C	56.5	61	48	56	59.5	45	1
M3H	52	59	35	45.5	53.5	23	5.5
M6H	55.5	58.5	62	51.3	54	63	4
M11H	55	57.3	27	54.5	57	43	0.5
M3E	—	57	1.2	—	55	1.2	—
M6E	—	57	2.6	—	53.6	2.3	2
M11E	—	58	6	—	57	5	2

[a] Temperature for 10% transmittance of cells.
[b] Phase change temperature from nematic to isotropic.
[c] Temperature hysteresis for 50% transmittance before and after UV irradiation.

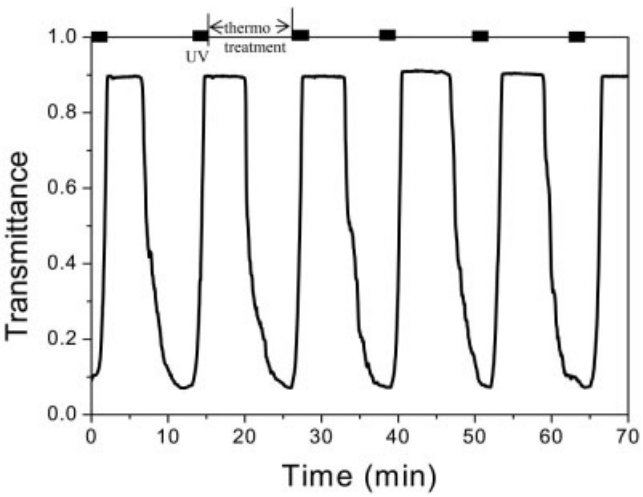

Figure 11 Stability and reliability of PDLC cells.

proposed. The clearing point of MnH decreased as the alkyl chain length increased; this means MnH as an impurity was doped in the liquid crystal phase and we found MnH series took a much longer time to dissolve in the liquid crystal solution than others. All of the samples have a little higher transmittance after we began UV light irradiation. This was because the *cis*-azobenzene formed and disturbed the alignment of the liquid crystal, which decreased the scattering of each liquid crystal domain to bring about the transmittance increase. The shorter alkyl chain length of azobenzene model compound doped in the PDLC films had a larger temperature hysteresis than the longer one. The sample containing M3C had the largest temperature hysteresis, at about 12°C. The model compound of the azobenzene monomer showed a higher contrast ratio and higher temperature hysteresis.

Figure 11 shows the reversible isomerization property of sample M6C operating at 57°C. The sample was irradiated with UV light for 3 min and then the light was turned off for 10 min repeatedly. The transmittance rises up to saturation state within 100 s. This was coincident with the value observed in solution. This may be because the liquid crystal contained 80 wt % and the azo compound contained 4.6–6.4 wt % and still had higher free isomerization space in the sample. After the UV light irradiation, the sample still maintained higher transparency for at least 4 min. Within this time, although some *cis*-form isomerized to its *trans*-form, the liquid crystal molecules remained at the isotropic state. After 4 min the transparency decreased dramatically and then maintained a 9% transparency; this result was coincident with the result in Figure 9(d). The *cis*-form azobenzene compound almost isomerized to its related *trans*-form within 10 min at 57°C. We speculated this is faster than we observed at room temperature as Figure 7(b) shows. The higher the temperature, the faster the *cis* → *trans* isomerization, and when we elevated the temperature to 80°C, the recorded image could be erased to its original highly scattering state within 3 min. The higher the temperature, the faster the *cis*-form azobenzene molecule isomerized to its stable *trans*-from azobenzene. The reversibility of azobenzene-doped PDLC samples can be used as optical switchable windows or image recorded materials.[20,21]

Using the property described above, we irradiated UV light through a mask on PDLC samples doped with M6H. The dark area prevented the UV light from passing through the sample so the area still maintained nematic liquid crystal properties in each liquid crystal domain and led the incident light to be highly scattered. The transparent area of the mask let the UV light pass through and decreased the clearing temperature so the area could allow incident light to pass through. We put a black paper under the PDLC sample so the dark part was the area irradiated with UV light and the other area was scattered light, which could not be seen through the sample and showed the color of azobezene compound. Figure 12 shows the reversible recorded image of PDLC films doped with M6H.

All the PDLC compositions investigated were examined by SEM. Figure 13 shows SEM photographs of PDLC films after removal of the liquid crystal by extraction with *n*-hexane. Many chinks containing liquid crystal were observed. Such structures have larger memory effects than structures with liquid crystal formed droplets interconnected in the polymer matrix.[9] The morphology of all these PDLC samples containing azobenzene were almost the same; we speculate that the different electric–optical properties be-

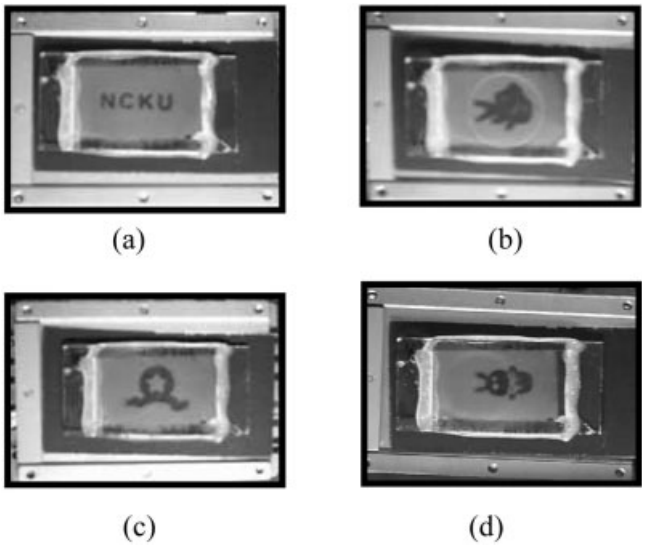

Figure 12 Image recording of PDLC cells by UV irradiation through masks.

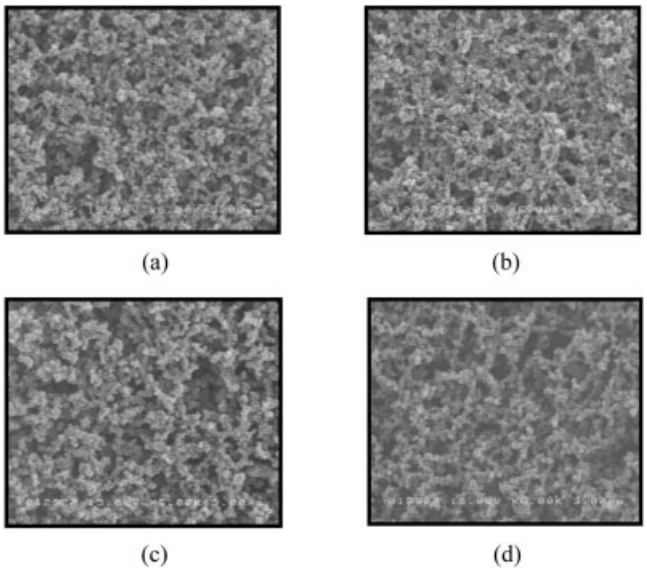

Figure 13 SEM photographs of PDLC film with various azobenzene derivatives of (a) M3E, (b) M6E, (c) M11H, and (d) M12C.

tween monomers and small molecules were caused by the situation of azobenzene molecules connected to the polymer matrix or dispersed in the liquid crystal domain; meanwhile, the flexibility derived from the alkyl chain length connected to the azobenzene molecules also had an important effect on the electric–optical properties.

CONCLUSION

We synthesized methoxy end-caped azobenzene monomers and their related model compounds with methyl or hydroxy end groups and changed the various alkyl chain lengths used in the field of the PDLC films. We found different electric–optical properties between monomers and their related model compounds. We proposed a model to explain these experimental phenomena. The sample was highly scattered and had a higher CR. The photoisomerization process was confirmed by UV-vis spectroscopy and it followed the mechanism of the isomerization mechanism. The sample showed a large clearing temperature, which declined when irradiated with UV light, and we used this unique property to record image. The repeatable property was confirmed and the image was successfully recorded by the experiment. The morphology was analyzed by SEM and showed that LC lied in the chinks domain.

The authors thank the National Science Council (NSC) of the Republic of China (Taiwan) for financially supporting this research under Contract No. NSC 92–2216-E006–005.

References

1. Bouteller, L.; Barny, P. L. Liq Cryst 1996, 21, 157.
2. Petti, L.; Mormile, P.; Blau, W. J. Opt Lasers Eng 2003, 39, 369.
3. Mormile, P.; Musto, P.; Petti, L.; Ragosta, G.; Villano, P. Appl Phys B 2000, 70, 249.
4. Doane, J. W.; Vaz, N. A.; Wu, B. G.; Zumer, S. Appl Phys Lett 1986, 48, 4, 269.
5. Lin, H.; Ding, H.; Kelly, J. R.; Mol Cryst Liq Cryst 1995, 262, 99.
6. Khow, I. C.; Wu, S. T. Optics and Nonlinear Optics of Liquid Crystals; Utopia Press: Singapore, 1993; Vol. 1, Chapter 2.
7. Wu, J. J.; Wang, C. M.; Chen, S. H. Jpn J Appl Phys 1996, 35, 2681.
8. Lee, S. H.; Lim, T. K.; Shin, S. T.; Park, K. S. Jpn J Appl Phys 2002, 41, 208.
9. Yamaguchi, R.; Sato, S. Jpn J Appl Phys 1991, 30, L616.
10. Nose, T.; Masuda, S.; Sato, S. Jpn J Appl Phys 1991, 30, 3450.
11. Fuh, A. Y. G.; Ko, T. C.; Li, M. H. Jpn J Appl Phys 1992, 31, 3366.
12. Viswanathan, N. K.; Kim, D. Y.; Bian, S.; Williams, J.; Liu, W.; Li, L.; Samuelson, L.; Kumar, J.; Tripathy, S. K. J Mater Chem 1999, 9 1941.
13. Natasohn, A.; Rochon, P. Chem Rev 2002, 102, 4139.
14. Yaroshchuk, O. V.; Kiselev, A. D.; Zakrevskyy, Y.; Bidna, T.; Kelly, J.; Chien, L. C. J Phys Rev 2003, 68, 11803.
15. Angeloni, A. S.; Caretti, D.; Carlini, C. Liq Cryst 1989, 4, 513.
16. Silong, S.; Lutfor, M. R.; Rahman, M. Z. A.; Yunus, W. M.; Haron, M. J.; Ahmad, M. B.; Yusoff, W. M. J Appl Polym Sci 2002, 86, 2653.
17. Yamaguchi, R.; Sato, S. Jpn J Appl Phys 1994, 33, 4007.
18. Wu, J. J.; Wang, C. M.; Li, W. Y.; Chen, S. H. Jpn J Appl Phys 1998, 12A, 6434.
19. Altomare, A.; Carlini, C.; Ciardelli, F.; Solaro, R. Polymer 1983, 24, 95.
20. Liu, J. H.; Wang, H. Y. J Appl Polym Sci 2004, 91, 789.
21. Liu, J. H.; Yang, P. C. J Appl Polym Sci 2004, 91, 3693.